# Crash-worthiness Analysis of Hollow Hybrid Structural Tube by Aluminum with Basalt-Bamboo Hybrid Fiber Laminates by Roll Wrapping Method

Padmanabhan Rengaiyah Govindarajan,[a] Rajesh Shanmugavel,[b,]* Sivasubramanian Palanisamy,[c,]* Tabrej Khan,[d] and Omar Shabbir Ahmed [d]

Hollow hybrid structural tubes were evaluated using commercial-grade Diamond Micro Expanded Mesh (DMEM) thin mesh of aluminum (Al) as structural reinforcement. Axial, transverse (flexural), and radial compression tests were performed on four different layered hybrid structures using bamboo (Bm) and basalt (B). With a maximum force of 34.7 kN, compressive ultimate strength of 238 MPa, and strain of 12.6%, AlBmB (with layers labeled from inside to outside) was the best performer in the axial compression test. AlBmB's adaptability was demonstrated by the flexural test, showing a maximum bending force of 4.7 kN, a flexural strength of 97.7 MPa, and a decreased deflection of 13.2 mm. Radial compression test results underscored the superior energy absorption characteristics of AlBmB. The varying material interfaces in the hybrid tubes yielded distinctive performances. AlBmB, incorporating bamboo and basalt layers, stood out with superior energy absorption and crush force characteristics, indicating enhanced crashworthiness. The other hybrids AlBm, AlB, and BmB also exhibited commendable performances, emphasizing the adaptability of different material combinations. The meticulous selection of DMEM and innovative roll wrapping method for fabrication reliably influenced the tubes' mechanical properties. The study contributes to advancing the design of lightweight, durable, and high-strength components.

*DOI: 10.15376/biores.19.2.3106-3120*

*Keywords: Hollow hybrid structure; Basalt; Bamboo; Polymer laminates; Roll wrapping method; Axial compression; Radial compression*

*Contact information: a: Department of Automobile Engineering, Kalasalingam Academy of Research and Education (KARE), Krishnankoil, Srivilliputhur – 626126, Tamil Nadu, India; b: Department of Mechanical Engineering, Kalasalingam Academy of Research and Education, (KARE), Krishnankoil, Srivilliputhur – 626126, Tamil Nadu, India; c: Department of Mechanical Engineering, P T R College of Engineering & Technology, Thanapandiyan Nagar, Madurai-Tirumangalam Road, Madurai, 625008, Tamilnadu, India; d: Department of Engineering Management, College of Engineering, Prince Sultan University, Riyadh- 11586, Saudi Arabia;*
** Corresponding authors: s.rajesh@klu.ac.in; sivaresearch948@gmail.com*

## INTRODUCTION

Because of several significant developments, environmental factors are receiving increased attention in modern manufacturing engineering. Growing global consumerism highlights how important it is to choose materials carefully when making products, as this has led to considerable advancements in a variety of industrial fields. Babazadeh *et al.* (2021), studied the selection of materials and the choices of manufacturing techniques and methods, which prove to be crucial factors that have an immediate impact on production schedules, costs, and the environmental impact of the processing. This focus on choosing materials and processes carefully not only considers the environmental issues but also fits in with the need to maximize sustainability and efficiency in industrial production models (Babazadeh *et al*. 2021; Arumugam *et al.* 2022). A strategic response to current issues is reflected in the integration of modern materials and production techniques, which is reshaping industrial operations in the direction of resource and environmentally conscious methods (Mache *et al*. 2020).

Composites are extensively utilized in the production of tubes, namely within sectors including petroleum, chemical plants, and aerospace. These composite tubes are comprised of a thermoset resin-based material with a fibre reinforcement, resulting in corrosion-resistant, lightweight, and solid structures. As a result, they are exceedingly favoured alternatives to conventional metal and concrete tubes. Ongoing studies investigate the utilization of various resin-based materials—specifically, Swancor-901, Epiran-1012, and Epiran-06FL—in the fabrication of composite tubes. The resins are reinforced with a variety of fibres, such as carbon, glass, and Kevlar, in accordance with their designated functions (Tabrej *et al*. 2018; Mache *et al*. 2020). This reinforcement is achieved in both unidirectional and 45° angle configurations. The winding process ensures that the dimensions, thickness, and diameter of the manufactured composite tubes are consistent. To evaluate the mechanical characteristics of the manufactured composite tubes, a battery of experiments was carried out, which included tensile, compressive, and three-point flexural strength tests.

According to prior studies, the performance of aluminum-carbon fiber reinforced polymer (Al/CFRP) hybrid tubes is significantly influenced by the interfacial bond strength between materials, specifically when subjected to shear stress (Zhou *et al*. 2021). Weak interfacial connections have the potential to cause debonding and delamination, which can significantly impair the effectiveness of the high-strength CFRP layer in reinforcing Al tubes. This is particularly true when shear stress is applied. Therefore, there is a primary concern with reducing the probability of peeling and delamination (Khan *et al*. 2018; Ma *et al*. 2021, 2022; Padmanabhan *et al.* 2022).

The concept of "bamboo woven fabric" relates to a unique manufacturing method that involves extracting and arranging bamboo fibres to form a woven structure that resembles fabric. The process starts by separating bamboo fibres from the plant, which is carried out through either pulping or mechanical processes. To improve the process of weaving, these fibres undergo processing to attain elongated filaments that are well-suited for traditional weaving processes. After the bamboo fabric is woven, it undergoes additional treatment specific to its purpose of manufacture by extraction process. The fibres are transformed into yarns or threads using specialised equipment (Kanaginahal *et al.* 2023).

The objective of this study was to provide valuable insights on the effectiveness and compatibility of various resin-fiber combinations in the production of composite tubes (Supian *et al*. 2018; Hanan *et al*. 2022; Palanisamy *et al*. 2023b). Eyer *et al*. (2016), studied compression tests and found that the failure mode of specimens can be influenced by factors such as slenderness. Excessive slenderness may lead to buckling affecting the failure, while less slender specimens may experience stress concentration and failure at the clamped end. In cases where structural effects play a significant role in failure, it becomes challenging to draw conclusions about the material's properties. To address this challenge, a solution lies in employing compression tests with dumbbell-shaped tubes. The use of such tube geometry provides a more controlled and standardized testing environment.

Dumbbell-shaped tubes offer advantages in terms of mitigating issues related to specimen slenderness, thus allowing for a more accurate assessment of material properties.

Additionally, these tubes enable the imposition of combined loads, such as shear/traction or shear/compression. Through adopting dumbbell-shaped tubes in compression testing, researchers and engineers can overcome challenges associated with specimen geometry, ensuring that the observed failure modes are more reflective of the material's intrinsic properties rather than structural effects (Sadasivuni *et al*. 2020; Palanisamy *et al*. 2024). This approach enhances the reliability and accuracy of material characterization, contributing to a better understanding of how materials respond under different loading conditions (Eyer *et al*. 2016). This will facilitate the selection of materials for diverse industrial applications in an optimum manner.

This study examined how intermediate diameter, wall thickness, and upper end diameter affect composite, metal, foam-filled, and hybrid tube SEA (Alia *et al.* 2015). Quasi-static axial compression testing was used to determine glass fibre-reinforced polymer failure characteristics (GFRP). Experimental stress-strain curves for polyurethane and aluminium foam were developed (Kulhavy and Lepsik 2017). Finite element models were generated for hollow GFRP, aluminium, aluminium-FRP, polyurethane foam-filled, and aluminium foam-filled composite tubes. Numerical models included round, square, and tapered tubes with five upper end sizes (Zhang *et al*. 2018; Kurien *et al*. 2023; Sumesh *et al*. 2023).

In this research work, HSS tubes were fabricated by roll wrapping techniques by four difference stacking specimens, namely - a) AlBm, b) AlBmB, c) AlB, and d) BmB. These specimens were produced, based on Al-DMEM (Al) as metal reinforced with bamboo woven (Bm) as natural fibre, basalt woven (B) fibre as hybrid fibre with epoxy resin. By various stacking arrangements, investigation of HHS tubes was performed with crashworthiness analysis by axial, flexural, and radial compression testing.

## EXPERIMENTAL

### Materials and Fabrication Methods

In the fabrication of HHS tube through the roll wrapping method, a specific combination of metal laminates including aluminum-DMEM alloys (Georgantzia *et al*. 2021), bamboo fibers (Bm) (Kumar *et al*. 2021; Sivasubramanian *et al*. 2021), and basalt fibers (B), was employed to create composite structures with superior mechanical properties, in accordance with Table 2. The structural reinforcement of metal as Al-DMEM thin mesh as commercial-grade aluminum 6061 alloy mesh with dimensions of SWD 2 mm, LWD 4 mm, and a thickness of 0.9 mm as shown in Table 2, were fabricated. This mesh was strategically positioned as the inner layer, ensuring optimal reinforcement within the composite structure as indicated in Fig. 1. Subsequently, the bamboo yarns were efficiently interwoven using standard techniques such as plain weave, which makes a woven fabric that exhibits the intended pattern and texture. The addition of the woven bamboo layer improved the strength, durability, and aesthetic appeal of composite buildings. Consequently, it is vital in hybrid material assemblies to enhance their durability and appearance. Bamboo fibers in the middle layer serve as more than spacers. They resist inward collapse under pressure or compressive loads due to their tensile strength and stiffness (Safwan *et al.* 2018). Bamboo fibers absorb and distribute impact energy, improving durability and impact resistance. Their lightweight and corrosion-resistant characteristics reduce weight and environmental impact without affecting performance. Bamboo fibers in the middle layer strengthen the tube, enhance impact resistance, reduce weight, and improve environmental durability, extending its lifespan.

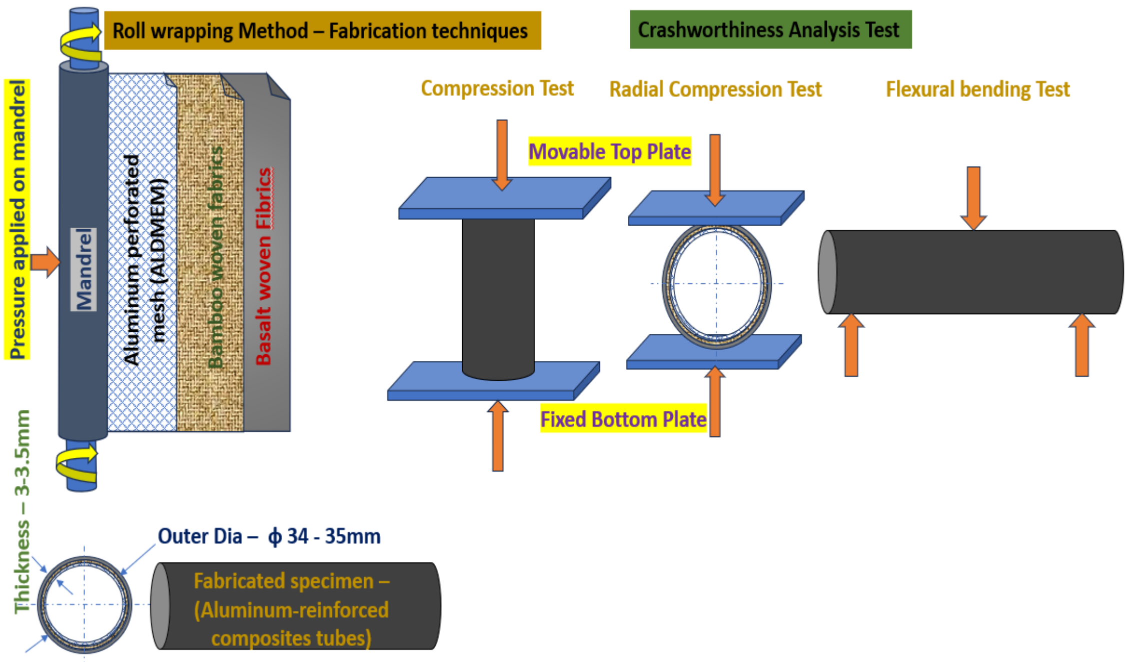


**Fig. 1.** Fabrication techniques and testing specimens

The roll wrapping process involves the utilization of an HHS tube with dimensions of 450 × 35 × 3 mm$^3$ as the foundational structure. A matrix for the composite was meticulously crafted using a resin system comprising regular epoxy LY 556 and HY 951 as a hardener, mixed precisely in a ratio of 10:1. Epoxy mixes are flexible before curing, which allowed easier assembly of the basalt with the bamboo woven fiber composites with ALDMEM. This delay in hardening allowed component alignment and positioning. Then the epoxy cured and strengthened the composite. Then the specimens were equilibrated for 4 to 8 hours at the environmental temperature. In addition, as a means to achieve high strength in bonding, post curing was done for 3 hours in a 150 °C oven.

During the roll wrapping process, the Al-DMEM mesh acted as the inner layer in the AlBm sample, with bamboo woven fabric applied as the outer layer. The AlBmB sample introduced an additional layer of bamboo woven fabric between the Al-DMEM mesh and basalt woven layer. The AlB sample featured the Al-DMEM mesh as the inner layer and basalt woven fabric as the outer layer. In the BmB sample, bamboo woven fabric was the inner layer, complemented by basalt woven fabric as the outer layer from Table 1. Epoxy resin is meticulously applied throughout the layering process to ensure structural integrity and bonding. Bamboo and basalt fibers, sourced from Go Green Products Private Limited, Chennai, were selected for their strength, durability, and sustainable properties. The result is a comprehensively fabricated set of hybrid structural tubes exhibiting enhanced mechanical properties (Suresh and Jayakumari 2016), making them suitable for a wide array of engineering applications in micromobility frames.

## Crashworthiness Indicators

In the field of structural mechanics, the quantification of energy absorption is a recognized approach for evaluating the crashworthiness of materials and structures (Ma *et al*. 2022). The energy absorption (EA) indicator can be defined as the integral of force for displacement during axial crushing (Ye *et al.* 2020), expressed mathematically in Eq. 1,

$$EA = \int Fd\delta \tag{1}$$

where $F$ represents the crushing force (kN), and $\delta$ signifies the crushing distance (mm), providing a quantitative measure of the energy dissipation capabilities under axial loads. Specific energy absorption (SEA) refines this evaluation by introducing a normalized ratio of absorbed energy to the total mass ($m$) of the structure. Mathematically,

$$SEA = (\int Fd\delta)/m \tag{2}$$

Equation 2 enables comparative analyses across various energy absorbers. Mean crush force (MCF) further standardizes the assessment by incorporating both absorbed energy (EA) and crushing distance ($\delta$), yielding Eq. 3:

$$MCF = SEA/\delta \tag{3}$$

Crush force efficiency (CFE), a pivotal parameter, delineates the efficiency of an energy absorber through the ratio of mean crushing force ($F_m$) to peak crushing force ($F_p$), expressed in Eq. 4:

$$CFE = \frac{F_m}{F_p} \tag{4}$$

From Eq. 4, an optimal energy absorber achieves a CFE of 100%, indicating parity between mean and peak crushing forces. Collectively, these technical indicators furnish a comprehensive framework for the meticulous assessment and comparative analysis of crashworthiness characteristics in materials and structures, which are crucial for ensuring optimal performance and safety in diverse engineering applications (Kar *et al*. 2023).

Reinforced composites, especially FRP, are in high demand. Veeresh Kumar *et al*. (2021) stated that the natural fibres have lower density and cost than glass fibres. While the natural fibers in this study share properties with glass fibers in certain aspects, such as density and cost savings, they exhibit relatively lower strength. Bamboo fibers, woven as fabric, were utilized to construct a polymer composite in this investigation. Rollers apply uniform pressure to impregnate fibres with adhesive resin. The study uses bamboo fibres as reinforcement to take use of natural fibres' benefits while admitting their limitations compared to glass fibres. This technique addresses the growing interest in ecological and cost-effective composite materials (Kumar *et al*. 2021; Neto *et al*. 2022; Palanisamy *et al*. 2023a). Zhang *et al*. (2018) investigated the composite tubes as energy-absorbing substitutes for metal structures in automotive, aerospace, and transportation applications.

## Axial Compression Test

In the assessment of the fabricated tubes' compressive strength, axial compression tests followed the established ASTM D5449 (2018) standard, following the approach illustrated in Fig. 1. This standardized procedure involved subjecting the tubes to compressive forces at a consistent speed of 5 mm/min under ambient temperature conditions, aiming to comprehensively evaluate the tubes' resistance and deformation characteristics under axial loading conditions from Fig. 2.

**Table 1.** The Feature and Layers of Fibers for the Production HHS Tubes

| S. No. | Material Combination | Sample Code | Resin | Inner (Each 1 Layer) | Middle (Each 1 Layer) | Outer (Each 1 Layer) |
|---|---|---|---|---|---|---|
| 1. | Aluminum + Bamboo | AlBm | Epoxy | Al-DMEM mesh | - | Bamboo Woven |
| 2. | Aluminum + Bamboo + Basalt | AlBmB | Epoxy | Al-DMEM mesh | Bamboo Woven | Basalt Woven |
| 3. | Aluminum + Basalt | AlB | Epoxy | Al-DMEM mesh | - | Basalt Woven |
| 4. | Bamboo + Basalt | BmB | Epoxy | Bamboo Woven | - | Basalt Woven |

**Table 2.** Materials Compositions

| Materials | Lignin (wt%) | Hemi-cellulose (wt%) | Cellulose (wt%) | Moisture (wt%) | Density (g/cm³) | Thickness (mm) | Surface Density (g/m²) | Type |
|---|---|---|---|---|---|---|---|---|
| **Bamboo** | 27 | 26 | 46 | 11 | 0.5 | 0.6 | 250 | Woven |
| **Basalt** | - | - | - | - | 2.8 | 0.8 | 350 | Woven |
| **Al-DMEM 6061** | - | - | - | - | 1.8 | 0.9 | 650 | mesh |
| **Al-DMEM 6061 Composition** | | | | | | | | |
| | **Al** | **Cu** | **Mg** | **Mn** | **Cr** | **Fe** | **Zn** | **Si** |
| **% Values** | 95.6% to 98.9% | 0.13% to 0.6% | 0.9% to 1.3% | 0.16% max | 0.04% to 0.38% | 0.6% max | 0.27% max | 0.3% to 0.7% |

## Material Testing

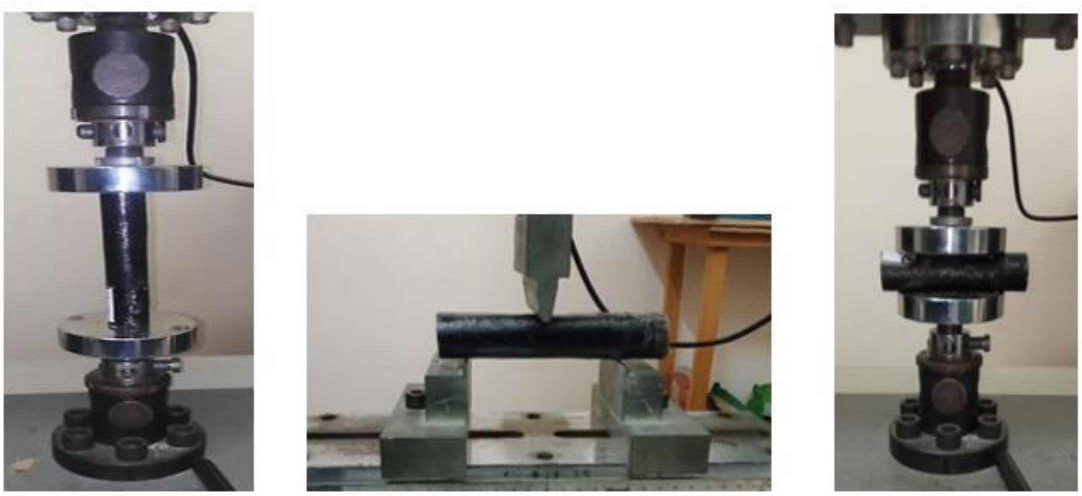

a b c

**Fig. 2.** Specimens for crashworthiness test – a: Axial compression test, b: Transverse Compression (Flexural) Test; and c: Radial compression test

The tubes selected for the compressive testing exhibited specific dimensional attributes, featuring a length of 60 mm, a thickness ranging from 3 to 3.5 mm, and a diameter within the range of 34 to 35 mm. The axial compression test, adhering to both ASTM D5449 (2018) and Heckadka *et al.* (2018) standards, entailed subjecting the tubes to controlled compressive forces, providing invaluable insights into their compressive strength and behavioral responses. The carefully specified dimensions ensure a meticulous evaluation of the tubes' structural performance and load-bearing capacities (Rouzegar *et al*. 2018). In axial compression tests on hybrid structural tubes combining bamboo and ALDMEM mesh with a basalt woven outer layer, forms a crumple-resistant structure relative to compressive failure. During standard axial compression tests, tubes undergo axial compressive forces until failure occurs. The failure mode may manifest itself as a crumpling collapse, where significant deformation and crushing resemble a crumpled structure (Zhu *et al*. 2020). This comprehensive evaluation, bolstered by adherence to ASTM D5449 standards, underscores the robustness and reliability of the conducted tests, reinforcing the credibility of the obtained results in informing engineering and material selection decisions (Ye *et al*. 2020).

## Transverse Compression (Flexural) Test

This test serves as a pivotal assessment method to ascertain the maximum fracture force and flexural strength of the produced HHS tubes, offering crucial insights into their mechanical properties (Ishak *et al.* 2010). Transverse compression test observes the ASTM D790 (2010) standard for evaluating the flexural behavior of materials. The 4 specimens selected for this analysis exhibited specific dimensions: a length of 300 mm, a thickness ranging from 3 to 3.5 mm, and a diameter within the range of 34 to 35 mm (Fig. 2). Notably, the supports are strategically positioned at a distance of 200 mm, aligning with the ASTM D790 (2010) standard requirements (Lv *et al.* 2019). The three-point flexural test involves the controlled application of force at a speed of 5 mm/min until the outer surface of the specimen ruptures. Flexural failure is precisely determined by monitoring the force-displacement curve, identifying the point where it reaches its maximum value. The flexural strength, a critical parameter in material characterization, is then calculated based on the maximum force applied and relevant relations (Gowid *et al*. 2020). Figure 2 provides a visual representation of the tubes undergoing the three-point flexural test, capturing the structural response under applied forces (Yin *et al*. 2020). The samples utilized in this comprehensive test correspond to the diverse material combinations outlined earlier, such as AlBm, AlBmB, AlB, and BmB. These combinations encompass varying configurations of aluminum, bamboo, and basalt components, facilitating a comprehensive assessment of their flexural characteristics and performance.

## Radial Compression Test

The radial compression testing of the tubes involves a thorough evaluation of material properties according to the stringent ASTM D2412 (2016) standards from Fig. 2, ensuring a robust and standardized testing protocol (Firouzsalari *et al*. 2020). The tubes, featuring specific dimensions of 60 mm length, 3 to 3.5 mm thickness, and 34 to 35 mm diameter, undergo comprehensive assessments to determine critical parameters such as energy absorption (EA), specific energy absorption (SEA), mean crush force (MCF), crush force efficiency (CFE), and peak crushing force (PCF). Adhering to the ASTM D2412 (2016) standards establishes a reliable and consistent approach, providing a standardized framework for evaluating the material's energy absorption capabilities and structural integrity under radial compression.

This extensive testing approach ensures that with industry standards, facilitating accurate and reproducible assessments of the tubes' radial compression performance. The specified parameters offer valuable insights into the tubes' behavior when subjected to radial forces, allowing for a comprehensive understanding of their energy absorption characteristics (Supian *et al*. 2020). The rigorous evaluation under ASTM D2412 (2016) ensures that the results obtained are not only precise but also comparable, contributing to the reliability of the findings in assessing the radial compression performance of the tubes (Bakar *et al.* 2020). This approach ensures that the tubes' performance is evaluated in a manner consistent with industry standards, enabling meaningful comparisons and insights into their suitability for various applications.

Crashworthiness tests, including axial, transverse, and radial compressions, were conducted at the LMP Research and Development Lab in Erode. The tests employed a servo-hydraulic computerized universal testing machine (Kalpak – KIC-2-1000C, Serial Number 121101; Kalpak Instruments and Controls Pvt, Ltd., India) with interchangeable load cells and a 25 kN capacity. This setup from LMP Research and Development Lab ensured accurate evaluations of the tubes' structural performance under different loading conditions (Prasath *et al*. 2020).

## RESULTS AND DISCUSSION

### Axial Compressive Analysis

The axial compression tests revealed significant performance discrepancies among the fabricated HHS tubes. From Table 3, sample AlBm demonstrated a maximum compressive force of 25.3 KN, with an ultimate strength of 145.1 MPa and a strain of 10.3%. In contrast, AlBmB showcased superior performance, with a maximum force of 34.7 KN, an ultimate strength of 238 MPa, and a strain of 12.6%. Similarly, AlB and BmB samples displayed varying compressive forces of 31.2 and 27.5 KN, and ultimate strengths of 218.58 and 122.95 MPa, respectively. Additionally, the (EA) differed notably between the samples, ranging from 151 J for AlBm to 254 J for AlBmB, indicating variations in their crashworthiness characteristics.

**Table 3.** Axial Compressive Analysis

| Sample | Max. Comp. Force (kN) | Comp. Ultimate Strength (MPa) | Strain (%) | PCF (kN) | EA (J) | MCF (kN) | SEA (J/g) | CFE | Deflec-tion (δ) (mm) |
|---|---|---|---|---|---|---|---|---|---|
| AlBm | 25.3 | 145.08 | 10.28 | 31.06 | 151.2 | 25.3 | 7.9 | 0.64 | 5.3 |
| AlBmB | 34.7 | 237.78 | 12.65 | 44.87 | 253.6 | 34.7 | 11.6 | 0.81 | 3.8 |
| AlB | 31.2 | 218.58 | 9.54 | 38.31 | 223.2 | 31.2 | 9.3 | 0.78 | 3.4 |
| BmB | 27.5 | 122.95 | 9.53 | 33.56 | 134.7 | 27.5 | 8.7 | 0.51 | 4.5 |

Furthermore, the MCF ranged from 25.3 kN for AlBm to 34.7 kN for AlBmB, suggesting differences in their load-bearing capacities under compressive loads. Additionally, the SEA ranged from 7.9 J/g for AlBm to 11.6 J/g for AlBmB, further highlighting variations in their energy absorption efficiency. Lastly, the CFE varied between 0.64 for AlBm and 0.81 for AlBmB, indicating differences in their efficiency in dissipating energy during compression. Table 1 provides details on the material combinations and layers of fibers used in tube production. The composition of bamboo and basalt materials, as well as the ALDMEM mesh, includes key parameters such as lignin, hemicellulose, cellulose content, moisture, density, thickness, and surface density. The compressive tests, conducted following ASTM D5449 (2018), underlined the varying strengths and deformations exhibited by the tubes. These results underscore the importance of tailored material combinations and layering techniques in optimizing the crashworthiness characteristics of the hybrid structural tubes.

From Fig. 3, failure may result from buckling, which is characterized by sudden lateral deflection of the tube under compression. Failure in composite structures like these tubes may also involve delamination, especially if bonding between layers is weak or if discontinuities exist. Delamination, the separation of layers within the composite, significantly impacts structural integrity. Visual inspection, accompanied by microscopic analysis or non-destructive testing, may reveal specific failure mechanisms, including delamination, bending, or buckling.

## Transverse Compression (Flexural) Analysis

The mechanical behavior and failure mechanisms of the tested HSS tubes were examined. Results of transverse compression analysis are shown in Table 4. Examining the results for all four specimens, which include (Al), (Bm), and (B) components, exposes characteristics under bending forces. Specimen AlBm, composed of aluminum and bamboo, displayed a maximum bending force of 3.5 KN, corresponding to a flexural strength of 86.7 MPa and a deflection of 19.8 mm. Despite exhibiting lower flexural strength compared to the other samples, AlBm demonstrated a distinguished EA of 82.3 J, indicating its capacity to absorb significant energy before failure. The failure mechanism primarily involved bending and localized deformation, with minor delamination observed under high stress conditions. Similarly, specimens AlBmB, AlB, and BmB showcased varying degrees of flexural strength, deflection, and energy absorption. Remarkably, AlBmB exhibited superior performance with a higher maximum bending force of 4.7 KN and a flexural strength of 97.7 MPa, accompanied by a reduced deflection of 13.2 mm and a remarkable EA of 91.7 J. This suggests improved stiffness and energy absorption capabilities in AlBmB, attributed to its unique composition incorporating bamboo and basalt layers.

**Table 4.** Flexural Analysis

| Samples | Max. Bending Force (KN) | Flexural Strength (MPa) | Deflection (δ) (mm) | EA (J) | PCF (kN) | MCF (kN) | CFE | SEA (J/kg) |
|---|---|---|---|---|---|---|---|---|
| AlBm | 3.5 | 86.68 | 19.8 | 82.3 | 2.6 | 3.1 | 0.78 | 1.14 |
| AlBmB | 4.7 | 97.72 | 13.2 | 91.7 | 3.9 | 4.9 | 1.14 | 2.21 |
| AlB | 4.1 | 92.43 | 15.9 | 87.4 | 3.5 | 4.1 | 1.02 | 1.87 |
| BmB | 3.7 | 88.12 | 18.3 | 83.1 | 3.1 | 3.3 | 0.94 | 1.54 |

Failure mechanisms observed in the HSS tubes primarily involved bending and localized deformation, with some specimens exhibiting minor delamination or cracking under high stress conditions. Overall, from Fig. 3, the results underscore the importance of material composition, including aluminum, bamboo, and basalt, as well as the bonding mechanism, in determining the flexural behavior and crashworthiness characteristics of the hybrid structural tubes, offering valuable insights for their optimization in structural panels in automotive sector.

## Radial Compression Test

Based on specimen interfaces, the radial compression study provided results on the energy absorption characteristics of hybrid structural tubes (Table 5). With its layers of basalt and bamboo, AlBmB notably exhibited improved crashworthiness and performed better. This implies a strong possibility for applications that need strong impact resistance. In contrast, although AlBm and BmB provided excellent results, their capacities to absorb energy were marginally less than those of AlBmB. These changes highlight the complex relationship that exists between the performance of a structure and its material combinations. AlBm, which combines bamboo with aluminium, exhibited encouraging qualities that may indicate potential applicability in certain situations. Comparably, BmB, which combines basalt and bamboo, exhibited adaptability and suggests that it can be used in a variety of situations. These findings highlight how crucial it is to choose materials specifically for hybrid structural tubes to maximise their energy absorption capabilities. Through the implementation of these insights, designers can optimise performance in dynamic environments by strengthening the robustness and safety of micromobility frames and other related applications. Therefore, even though AlBmB was clearly the leader, the subtle differences in performance between AlBm and BmB highlight the necessity of carefully weighing material combinations to get the desired performance results.

**Table 5.** Energy Absorption Parameters of HSS Tubes at Different Interfaces by Radial Compression Test

| Samples | EA (J) | PCF (kN) | MCF (kN) | CFE | SEA (J/kg) |
|---|---|---|---|---|---|
| AlBm | 99.53 | 5.11 | 4.15 | 0.62 | 2.13 |
| AlBmB | 107.89 | 6.20 | 5.83 | 0.97 | 2.71 |
| AlB | 104.86 | 5.82 | 5.02 | 0.84 | 2.49 |
| BmB | 102.98 | 5.48 | 4.60 | 0.78 | 2.19 |

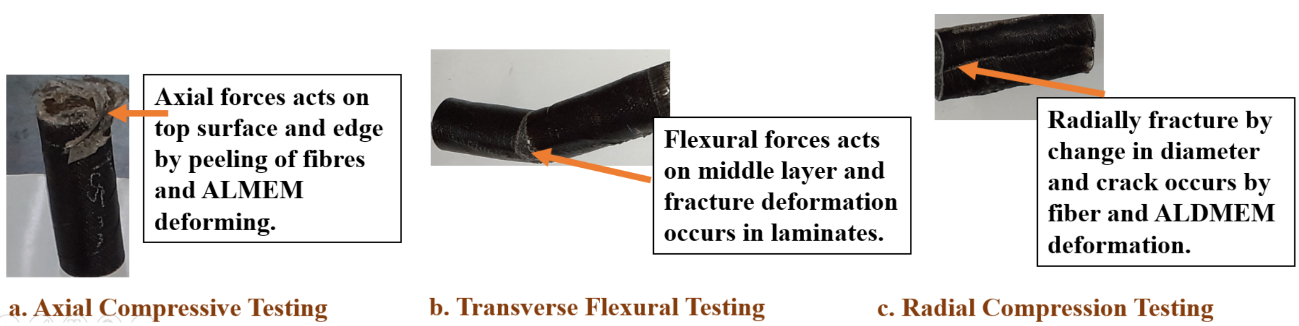


**Fig. 3.** Failure of HSS tube in three test analysis

## CONCLUSIONS

In conclusion, the evaluation of hybrid structural tubes through axial, transverse (flexural), and radial compression tests provided a comprehensive understanding of their mechanical behavior, emphasizing the impact of material combinations and layering configurations.

1. The AlBmB tube sample, having layers (from in to out) of aluminum, bamboo fiber, and basalt, in an epoxy matrix, surpassed the other formats across all tests, exhibiting superior compressive strength (34.7 kN), impressive flexural resistance (4.7 kN), and outstanding energy absorption (108). It exhibited superior performance, showcasing the efficacy of incorporating bamboo and basalt layers.
2. In the Axial Compressive Analysis, significant variations in crashworthiness were evident among the specimens, with AlBmB exhibiting superior performance due to its higher maximum compressive force and energy absorption. The failure mechanisms, including crumpling and localized deformation, underlined the position of tailored material combinations and layering techniques in enhancing crashworthiness.
3. In the Transverse Compression (Flexural) Analysis, distinguished differences in crashworthiness were observed among the tested specimens, with AlBmB demonstrating superior performance in maximum bending force and energy absorption, suggesting improved structural integrity.
4. In the Radial Compression Test, AlBmB showed higher energy absorption and specific energy absorption, indicating better crashworthiness. Crumpling and buckling demonstrated the relevance of epoxy bonding and customised material combinations in crashworthiness.
5. The selection of materials, including aluminum, bamboo, and basalt, coupled with the advanced roll wrapping method for fabrication, significantly influenced the tubes' mechanical properties.
6. The roll-wrapping method ensured uniform layering and effective bonding, contributing to the observed strengths and deformations in the conducted tests. These findings highlight the adaptability of different material compositions and layering techniques, offering valuable insights for optimizing crashworthiness in hybrid structural tubes.
7. AlBmB, with its superior performance across all tests, emerged as a promising candidate for applications demanding a balance between strength and flexibility. The versatility showcased by AlBm, AlB, and BmB samples further emphasized the trade-offs between various material combinations.

Overall, the hybrid tubes exhibited remarkable potential for applications in micromobility frames, offering enhanced structural integrity, energy absorption, and safety. The tailored material configurations and fabrication methods contributed to the optimization of crashworthiness characteristics, making these hybrid structural tubes suitable for diverse engineering applications requiring lightweight, durable, and high-strength components.

## ACKNOWLEDGMENTS

The authors would like to acknowledge the support of Prince Sultan University, Riyadh for paying the Article Processing Charge (APC) of this publication.

### Data Availability Statement

Data is available on request from the authors.

### Declaration of Conflicting Interests

The authors declared no potential conflicts of interest with respect to the research, authorship, and/or publication of this article.

## REFERENCES CITED

Abu Bakar, M. S., Salit, M. S., Mohamad Yusoff, M. Z., Zainudin, E. S., and Ya, H. H. (2020). "The crashworthiness performance of stacking sequence on filament wound hybrid composite energy absorption tube subjected to quasi-static compression load," *Journal of Materials Research and Technology* 9(1), 654-666. DOI: 10.1016/j.jmrt.2019.11.006

Alia, R., Guan, Z., Umer, R., and Cantwell, W. (2015). "The energy-absorbing properties of internally reinforced composite-metal cylinders with various diameter-to-thickness ratios," *Journal of Reinforced Plastics and Composites* 34(9), 731-741. DOI: 10.1177/0731684415579213

Arumugam, S., Kandasamy, J., Venkatesan, S., Murugan, R., Lakshmi Narayanan, V., Sultan, M. T. H., Shahar, F. S., Shah, A. U. M., Khan, T., and Sebaey, T. A. (2022). "A review on the effect of fabric reinforcement on strength enhancement of natural fiber composites," *Materials* 15(9), article 3025. DOI: 10.3390/ma15093025

Babazadeh, J., Rahmani, K., Hashemi, S. J., and Sadooghi, A. (2021). "Effect of glass, carbon, and kevlar fibers on mechanical properties for polymeric composite tubes produced by a unidirectional winding method," *Materials Research Express* 8(4), article ID 045301. DOI: 10.1088/2053-1591/abf0ba

Eyer, G., Montagnier, O., Charles, J. P., and Hochard, C. (2016). "Design of a composite tube to analyze the compressive behavior of CFRP," *Composites Part A: Applied Science and Manufacturing* 87, 115-122. DOI: 10.1016/j.compositesa.2016.04.006

Eyvazinejad Firouzsalari, S., Dizhur, D., Jayaraman, K., Chouw, N., and Ingham, J. M. (2020). "Flax fabric-reinforced epoxy pipes subjected to lateral compression," *Composite Structures* 244, article ID 112307. DOI: 10.1016/j.compstruct.2020.112307

Georgantzia, E., Gkantou, M., and Kamaris, G. S. (2021). "Aluminium alloys as structural material: A review of research," *Engineering Structures* 227, article ID 111372. DOI: 10.1016/j.engstruct.2020.111372

Gowid, S., Mahdi, E., Renno, J., Sassi, S., Kharmanda, G., and Shokry, A. (2020). "Experimental investigation of the crashworthiness performance of fiber and fiber steel-reinforced composites tubes," *Composite Structures* 251, article ID 112655. DOI: 10.1016/j.compstruct.2020.112655

Hanan, F., Khan, T., Jawaid, M., Sultan, M. T. H., Sebaey, T., Singh, B., and Sarmin, S. N. (2022). "Thermal characterization of epoxy bilayer hybrid composites reinforced with kenaf and oil palm fibers," *Polymer Composites* 44(1), 444-452. DOI: 10.1002/pc.27108

Heckadka, S. S., Nayak, S. Y., Vishal, S. P., and Amin, N. M. (2018). "Evaluation of flexural and compressive strength of e glass/jute and e glass/banana hybrid epoxy hollow composite shafts," *Key Engineering Materials* 777, 438-445. DOI: 10.4028/www.scientific.net/kem.777.438

Ishak, M. R., Leman, Z., Sapuan, S. M., Edeerozey, A. M. M., and Othman, I. S. (2010). "Mechanical properties of kenaf bast and core fiber reinforced unsaturated polyester composites," *IOP Conference Series: Materials Science and Engineering* 11, article ID 12006. DOI: 10.1088/1757-899X/11/1/012006

Kanaginahal, G. M., Hebbar, S., Shahapurkar, K., Alamir, M. A., Tirth, V., Alarifi, I. M., Sillanpaa, M., and Murthy, H. (2023). "Leverage of weave pattern and composite thickness on dynamic mechanical analysis, water absorption and flammability response of bamboo fabric/epoxy composites," *Heliyon* 9(1), article e12950. DOI: 10.1016/j.heliyon.2023.e12950

Kar, A., Saikia, D., Palanisamy, S., Santulli, C., Fragassa, C., and Thomas, S. (2023). "Effect of alkali treatment under ambient and heated conditions on the physicochemical, structural, morphological, and thermal properties of *Calamus tenuis* cane fibers," *Fibers* 11(11), article 92. DOI: 10.3390/fib11110092

Kulhavy, P., and Lepsik, P. (2017). "Comparison of modal characteristic of wrapped and winded composite tubes from carbon prepreg," *Vibroengineering Procedia* 11, 91-96. DOI: 10.21595/vp.2017.18545

Kurien, R. A., Selvaraj, D. P., Sekar, M., Koshy, C. P., Paul, C., Palanisamy, S., Santulli, C., and Kumar, P. (2023). "A comprehensive review on the mechanical, physical, and thermal properties of abaca fibre for their introduction into structural polymer composites," *Cellulose* 30(14), 8643-8664. DOI: 10.1007/s10570-023-05441-z

Lv, Y., Wu, X., Gao, M., Chen, J., Zhu, Y., Cheng, Q., and Chen, Y. (2019). "Flexural behavior of basalt fiber reinforced polymer tube confined coconut fiber reinforced concrete," *Advances in Materials Science and Engineering* 2019, article ID 1670478. DOI: 10.1155/2019/1670478

Ma, Q., Dong, F., Gan, X., and Zhou, T. (2021). "Effects of different interface conditions on energy absorption characteristics of Al/carbon fiber reinforced polymer hybrid structures for multiple loading conditions," *Polymer Composites* 42(6), 2838-2863. DOI: 10.1002/pc.26019

Ma, Q. H., Wang, K., Gan, X. H., and Tian, Y. X. (2021). "Optimization design in perforated AL-CFRP hybrid tubes under axial quasi-static loading," *International Journal of Crashworthiness* 27(5), 1317-1336. DOI: 10.1080/13588265.2021.1926852

Mache, A., Deb, A., and Gupta, N. (2020). "An experimental study on performance of jute-polyester composite tubes under axial and transverse impact loading," *Polymer Composite* 41(5), 1796-1812. DOI: 10.1002/pc.25498

Neto, J., Queiroz, H., Aguiar, R., Lima, R., Cavalcanti, D., and Doina Banea, M. (2022). "A review of recent advances in hybrid natural fiber reinforced polymer composites," *Journal of Renewable Materials* 10(3), 561-589. DOI: 10.32604/jrm.2022.017434

Padmanabhan, R. G., Karthikeyan, S., Parthasarathy, C., and Arockiam, A. J. (2022). "Crashworthiness test on hollow section structural (HSS) frame by metal fiber laminates with various geometrical shapes – Review," *AIP Conference Proceedings* 2520(1), article ID 0105050. DOI: 10.1063/5.0105050

Palanisamy, S., Kalimuthu, M., Dharmalingam, S., Alavudeen, A., Nagarajan, R., Ismail, S. O., Siengchin, S., Mohammad, F., and Al-Lohedan, H. A. (2023a). "Effects of fiber loadings and lengths on mechanical properties of *Sansevieria cylindrica* fiber reinforced natural rubber biocomposites," *Materials Research Express* 10(8), article ID 085503. DOI: 10.1088/2053-1591/acefb0

Palanisamy, S., Kalimuthu, M., Santulli, C., Palaniappan, M., Nagarajan, R., and Fragassa, C. (2023b). "Tailoring epoxy composites with *Acacia caesia* bark fibers: Evaluating the effects of fiber amount and length on material characteristics," *Fibers* 11(7), article 63. DOI: 10.3390/fib11070063

Palanisamy, S., Murugesan, T. M., Palaniappan, M., Santulli, C., Ayrilmis, N., and Alavudeen, A. (2024). "Selection and processing of natural fibers and nanocellulose for biocomposite applications: A brief review," *BioResources* 19(1), 1789-1813. DOI: 10.15376/biores.19.1.Palanisamy

Prasath, K. A., Arumugaprabu, V., Amuthakkannan, P., Manikandan, V., and Deepak Joel Johnson, R. (2020). "Low velocity impact, compression after impact and morphological studies on flax fiber reinforced with basalt powder filled composites. *Materials Research Express* 7(1), article ID 015317. DOI: 10.1088/2053-1591/ab611e

Rouzegar, J., Assaee, H., Elahi, S. M., and Asiaei, H. (2018). "Axial crushing of perforated metal and composite-metal tubes," *Journal of the Brazilian Society of Mechanical Sciences and Engineering* 40(7), article 349. DOI: 10.1007/s40430-018-1266-6

Sadasivuni, K. K., Saha, P., Adhikari, J., Deshmukh, K., Ahamed, M. B., and Cabibihan, J. (2020). "Recent advances in mechanical properties of biopolymer composites: A review," *Polymer Composites* 41(1), 32-59. DOI: 10.1002/pc.25356

Safwan, A., Jawaid, M., Sultan, M. T. H., and Hassan, A. (2018). "Preliminary study on tensile and impact properties of kenaf/bamboo fiber reinforced epoxy composites," *Journal of Renewable Materials* 6(5), 529-535. DOI: 10.7569/jrm.2018.634103

Sivasubramanian, P., Mayandi, K., Arumugaprabu, V., Rajini, N., and Rajesh, S. (2021). "History of composites," in: *Polymer-Based Composites: Design, Manufacturing, and Applications*, V. Arumugaprabu, R. Deepak Joel Johnson, M. Uthayakumar, and P. Sivaranjana (Eds.), CRC Press, Boca Raton, FL, USA, pp. 1-21. DOI: 10.1201/9781003126300

Sumesh, K. R., Ajithram, A., Palanisamy, S., and Kavimani, V. (2023). "Mechanical properties of ramie/flax hybrid natural fiber composites under different conditions," *Biomass Conversion and Biorefinery* 2023, (Online). DOI: 10.1007/s13399-023-04628-5

Supian, A., Sapuan, S., Zuhri, M., Zainudin, E., and Ya, H. (2018). "Hybrid reinforced thermoset polymer composite in energy absorption tube application: A review," *Defence Technology* 14(4), 291-305. DOI: 10.1016/j.dt.2018.04.004

Supian, A., Sapuan, S., Zuhri, M., Zainudin, E., and Ya, H. (2020). "Crashworthiness performance of hybrid kenaf/glass fiber reinforced epoxy tube on winding orientation effect under quasi-static compression load," *Defence Technology* 16(5), 1051-1061. DOI: 10.1016/j.dt.2019.11.012

Suresh, G., and Jayakumari, L. S. (2016). "Analyzing the mechanical behavior of E-glass fibre-reinforced interpenetrating polymer network composite pipe," *Journal of Composite Materials* 50(22), 3053-3061. DOI: 10.1177/0021998315615408

Veeresh Kumar, G. B., Kishore, C. N., Krishna Kanth, V., and Pramod, R. (2021). "Investigation on structural characteristics of bamboo-laminates," *IOP Conference Series: Materials Science and Engineering* 1185(1), article ID 012028. DOI: 10.1088/1757-899x/1185/1/012028

Ye, H., Zhou, X., Ma, J., Wang, H., and You, Z. (2020). "Axial crushing behaviors of composite pre-folded tubes made of KFRP/CFRP hybrid laminates," *Thin-Walled Structures* 149, article ID 106649. DOI: 10.1016/j.tws.2020.106649

Yin, D., Zheng, J., Xiong, C., Yin, J., Li, B., Deng, H., and Zhu, X. (2020). "Analytical, numerical, and experimental investigations on transverse bending responses of CFRP square tube filled with aluminum foam," *Mathematical Problems in Engineering* 2020, article ID 8764349. DOI: 10.1155/2020/8764349

Zhang, Z., Sun, W., Zhao, Y., and Hou, S. (2018). "Crashworthiness of different composite tubes by experiments and simulations," *Composites Part B: Engineering* 143, 86–95. DOI: 10.1016/j.compositesb.2018.01.021

Zhou, Q., Ma, Q., Zhou, T., and Gan, X. (2021). "The effects of interfacial connection condition on the characteristics of aluminum/CFRP hybrid tube under transverse quasi-static loading," *Fibers and Polymers* 22(6), 1761-1773. DOI: 10.1007/s12221-021-0498-8

Zhu, L., Lyu, L., Wang, Y., Qian, Y., Zhao, Y., Wei, C., and Guo, J. (2020). "Axial-compression performance and finite element analysis of a tubular three-dimensional-woven composite from a meso-structural approach," *Thin-Walled Structures* 157, article ID 107074. DOI: 10.1016/j.tws.2020.107074

Article submitted: February 17, 2024; Peer review completed: March 16, 2024; Revised version received: March 23, 2024; Accepted: March 24, 2024; Published: March 29, 2024.
DOI: 10.15376/biores.19.2.3106-3120